JOURNAL OF MATERIALS SCIENCE **38** (2003) 1787–1792

The effect of poling treatment and crystal structure of PZT on fracture toughness and fatigue resistance

WEON-PIL TAI
Institute of Advanced Materials, Inha University, Yonghyun-dong, Nam-ku, Inchon 402-751, South Korea

SONG-HEE KIM
Department of Materials Engineering and Science, Kangwon National University, Chunchon, Kangwondo, 200-701, Korea; Center for Advanced Aerospace Materials, POSTECH, Korea

Empirical measurements of fracture toughness and fatigue strength were conducted for piezoelectric $Pb(Zr_x,Ti_{1-x})O_3$ of various compositions such as tetragonal, MPB, and rhombohedral. Before the poling treatment the rhombohedral showed the highest fracture toughness, while the tetragonal revealed the lowest fracture toughness. After poling treatment, the fracture toughness measured by the pre-cracked SENB method decreased in all three compositions. The most remarkable decrease was observed in the tetragonal composition. However, when the indentation strength method was used the highest fracture toughness was observed in the tetragonal. The stress intensity factor relief due to microcracks around the indentation marks and the anisotropic internal stresses caused by domain alignment during the poling treatment were proposed as explanations for the comflicting results. Fatigue resistance was lowered by the compressive stress introduced during the poling treatment. The highest fatigue resistance was observed in the rhombohedral composition of low tetragonality, which exhibited low internal stress.

1. Introduction

Since Jaffe *et al.* [1] discovered higher piezoelectric properties near the tetragonal-rombohedral phase boundary in $Pb(Zr_x,Ti_{1-x})O_3$[PZT] ceramics, many attempts have been made to study the effects of additives and processing techniques to improve the piezoelectric properties [2, 3]. Piezoelectric properties can be attained in ferroelectric PZT ceramics by poling treatment. It is important to characterize the piezoelectric and mechanical properties of PZT ceramics, because these have been used as key materials for igniters, vibrators, transducers and sonar detectors, which are used under repeated deformation and stresses.

Ceramics generally show high strength and chemical stability, but brittleness, so the application of structural ceramics is often limited by low fracture toughness. However, insufficient work has been carried out to improve the fracture toughness evaluation of ceramics. In comparison with the studies on the mechanical properties of structural ceramics [4–6], less work has been performed in the case of ferroelectric ceramics [7–9]. Fracture toughness is one of the important mechanical properties of PZT ceramics, this is usually measured by either the indentation method [8] or the indentation strength method [9]. These methods, however, occasionally show large discrepancies in fracture toughness values because of inhomogeneous cracks and deformation around the indentation mark. Furthermore, Mehta and Virkar [10] measured the fracture toughness in unpoled and poled PZT by SENB (single edge notched beam) method, and the discrepancy of fracture toughness investigated in term of domain switching. Reece and Guiu [11] estimated that the upper limit (less than 10%) of the toughening produced by stress-induced domain switching at the tip of cracks in a ferroelectric/ferroelastic material was less than 10%. It is also important to understand the fatigue behavior of piezoelectric ceramics, because fatigue fracture gradually becomes prevalent during periods of use. Jiang *et al.* [12] and Cao *et al.* [13] studied electric fatigue in which the electric field was repeatedly applied. According to the authors knowledge, however, studies on fatigue behavior subject to mechanical cyclic loading have rarely been carried out, particularly for PZT ceramics. Thus the present research aims to evaluate the measurement methods for fracture toughness and studies on fatigue behavior and resistance for $Pb(Zr,Ti)O_3$ ceramics.

In the present study, a 3-point bending test using precracked SENB(single edge notched beam) specimens was conducted to measure the fracture toughness before and after poling treatment in tetragonal, Morphotropic Phase Boundary (MPB), and rhombohedral PZT, and the fracture mechanism has been discussed in terms of internal stress, domain switching, and microcracking.

The discrepancy between the different measurement methods for fracture toughness was discussed using a proposed model. Compressive cyclic loading was employed to study the effect of poling treatment and microstructure on the fatigue behavior of $Pb(Zr,Ti)O_3$, in which mechanism is discussed in terms of internal stress.

2. Experiments and materials

2.1. Sample preparation

The starting powders for the present investigation were PbO(Hayashi pure chemi., G.R.), ZrO_2 (Hayashi pure chemi., EP), and TiO_2 (Hayashi pure chemi., G.R.). The PZT samples (tetragonal [$Pb(Zr_{0.48}Ti_{0.52})O_3$], MPB [$Pb(Zr_{0.53}Ti_{0.47})O_3$], and rhombohedral [$Pb(Zr_{0.58}Ti_{0.42})O_3$]) were prepared by conventional ceramic processing. A mixture of the starting powders was milled and mixed in a vibratory mill. These oxide powders were homogenized in alcohol and calcined at 850°C for 3 hours. The calcined mixture was ball-milled and granulated. PVA was added as a binder to aid the formation of isostatically pressed compacts. It was added as a 1 wt% solution. The fine powder was isostatically pressed into rectangular bars of 5.5 mm × 7 mm × 28 mm and columnar types of 6 mm(Φ) × 12 mm(h) under 130 MPa. The bars were finally fired in covered alumina crucibles at 1280°C for 1 hour. Specimens were sintered in a $PbZrO_3$ + 5wt% ZrO_2 atmosphere to prevent the loss of PbO. The fired specimens were cut and ground to a bar type of 3.5 mm × 5 mm × 24 mm and a cylinder type of 5 mm(Φ) × 10 mm(h) with a diamond cutter, a diamond polishing wheel, and SiC abrasive paper(#1000, 1200). Poling treatment was carried out in silicone oil at 130°C for 9 min with the application of a DC electric field (2 kV/mm) parallel to the crack propagation direction. Fracture toughness specimens for a pre-cracked SENB method were prepared, having a notch width of 0.1 mm and a notch length of 2.3 mm. A realistic short pre-crack was artificially inserted from the machined notch tip in a direction perpendicular to the loading axis by applying cyclic compressive axial loading in a vertical direction [14, 15]. After the pre-cracking, fatigue crack propagation tests were conducted with three-point bending.

2.2. Measurements and analyses

The density of the sintered body was determined by the Archimedes method, and the grain size was measured by the linear intercept method [16]. X-ray diffraction (XRD) was used to determine the degree of domain switching from fracture surfaces. The internal stresses were evaluated by the inclination method using XRD and calculated by the following Equation 1 [17, 18]:

$$\frac{d_{\phi\varphi} - d_0}{d_0} = \frac{1+\nu}{E}\sigma_\phi \sin^2\varphi - \frac{\nu}{E}(\sigma_{11} + \sigma_{22}) \quad (1)$$

where σ_ϕ is the internal stress, $d_{\phi\varphi}$ is the stressed plane spacing, d_0 is the unstressed plane spacing, ν is Poisson's ratio, and E is Young's modulus.

Fracture toughness was evaluated using precracked SENB specimens with a lower span of 20 mm at a crosshead speed of 0.5 mm/min. Five or more specimens were tested under the same conditions. Sinusoidal loading at 20 Hz was selected for the cyclic compressive axial loading fatigue test. A load ratio ($R = \sigma_{\min}/\sigma_{\max}$) of 20 was maintained throughout the test, using a servo hydraulic dynamic testing machine (MTS Corp.).

3. Results and discussion

The microstructural analysis, densities and grain sizes of the PZT specimens are shown in Table I. Rhombohedral phases showed the finest grain size and the highest density.

Fig. 1 illustrates the change in fracture toughness values measured using precracked SENB specimens of various compositions before and after poling treatment. Before poling treatment, the highest fracture toughness was obtained in rhombohedral, while the tetragonal showed the lowest fracture toughness. After poling treatment, the fracture toughness decreased in all three compositions, and the most prominent decrease in fracture toughness occurred in the tetragonal composition. Before poling treatment, the highest fracture toughness in the rhombohedral composition was attributed to relatively greater density and smaller grain size. Mehta and Virkar [10] measured the fracture toughness of tetragonal PZT specimens using similar SENB specimens. The fracture toughness in the unpoled condition was higher than that in the poled condition, and the higher fracture toughness in the unpoled condition was explained in terms of domain switching at the instant of fracture. In the present study, XRD analyses were performed to investigate domain switching. It has been reported elsewhere [19] that the domain switching at the fracture under compressive stress was observed to be more remarkable in the poled specimens than in the unpoled ones, as seen in Fig. 2. However, a slight domain switching was found to occur near the fracture surface after the fracture toughness tests using 3-point bending, as shown in Fig. 3. More domain switching after the fracture under compressive stress was observed higher than that under tensile stress under 3-point bending.

The internal stresses of the unpoled and the poled PZT specimens were measured by an X-ray diffraction method as shown in Table 2. Isotropic internal stresses were exhibited in the unpoled specimens while, on the other hand, anisotropic internal stresses occurred in poled specimens. This indicates that compressive and tensile stresses were produced parallel and perpendicular to the poling direction, respectively, due to the poling treatment. However it has been accepted in general

TABLE I Microstructural properties of PZT ceramics, $Pb(Zr_x, Ti_{1-x})O_3$

Specimens	x	Phases	Density (g/cm^3)	Grain size (μm)
PZT48 (tetragonal)	0.48	T	7.55	14.5
PZT53 (MPB)	0.53	T + R	7.56	13.9
PZT58 (rhombohedral)	0.58	R	7.58	12.1

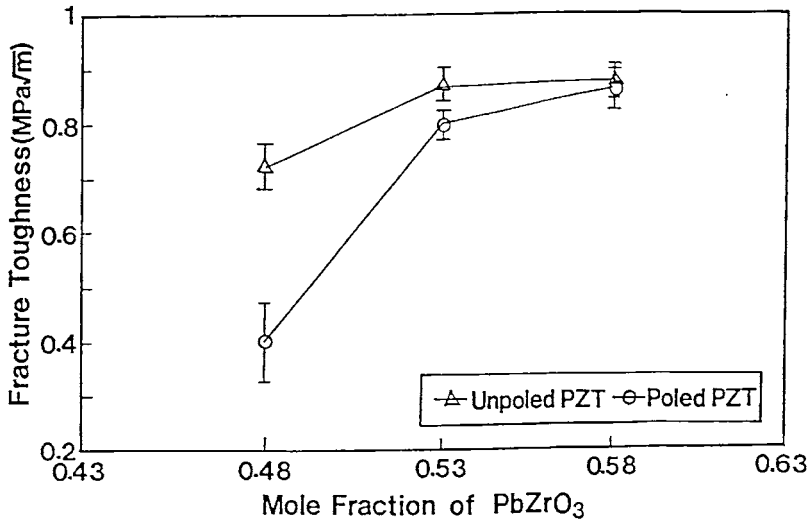

Figure 1 Fracture toughness of PZT measured by 3-point bending test using SENB specimens in three different compositions.

that the internal stresses measured by the XRD method do not show absolute accuracy but indicate the relative value. The microcracking caused by tetragonality (c/a − 1.029) during poling treatment has frequently been observed in the tetragonal composition. If a three-point bending load is applied to an SENB specimen having a microcrack in the tetragonal composition as shown in Fig. 4, the interaction of stresses in the left and right sides of the growing crack boundary and the tensile stress perpendicular to the poling direction can accelerate crack growth.

However, it has been reported in previous research [6, 20] that the fracture toughness was increased by the formation of microcracks. Where the microcrack-induced toughening is in effect, the fracture toughness will be increased by the microcracks after poling treatment. In spite of the occurrence of microcracking during poling, the fracture toughness decreased in working after the poling treatment. It is suggested that a large amount of fracture toughness of the poled specimen in the tetragonal composition was negated, firstly, by the tensile stress perpendicular to the poling direction, secondly, by the microcracks near the crack tip induced by the poling treatment, and thirdly, less domain switching at the fracture under tensile stress. The decrease in fracture toughness in poled MPB and rhombohedral compositions was attributed to the increase in internal tensile stress perpendicular to the crack propagation direction due to domain alignment.

Discrepancies in the fracture toughness measured by the precracked SENB and the indentation strength method are presented in Figs 1 and 5. In the precracked

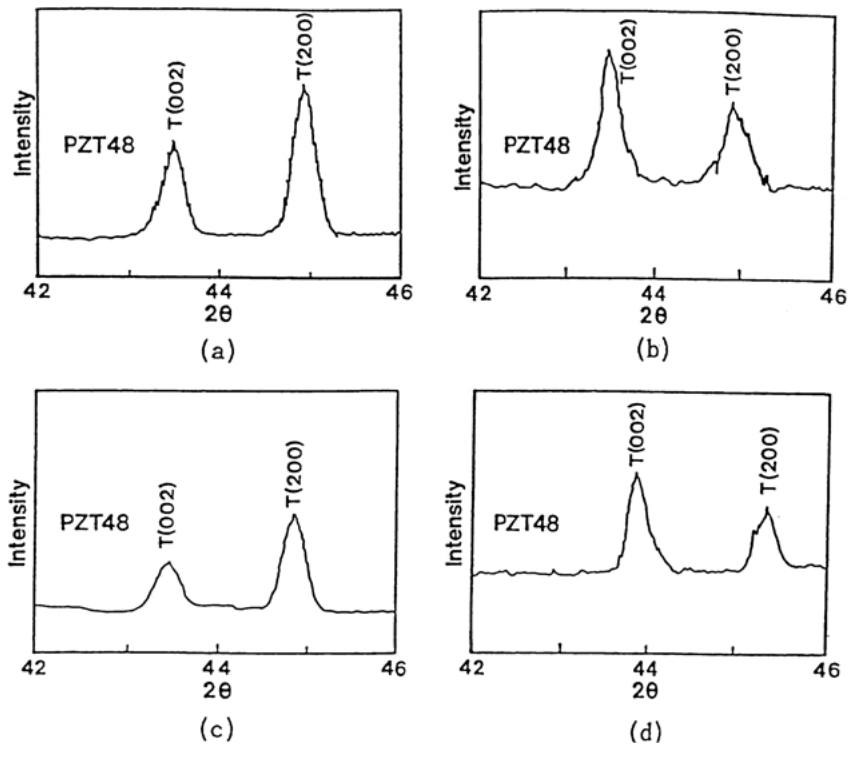

Figure 2 The change in X-ray diffraction patterns of tetragonal $Pb(Zr_{0.48}\ Ti_{0.52})O_3$ before and after poling treatment: (a) surface of unpoled condition ($I_{(002)}/I_{(200)} = 0.67$), (b) fracture surface of unpoled condition ($I_{(002)}/I_{(200)} = 1.84$), (c) surface of direction perpendicular to electric field, poled condition ($I_{(002)}/I_{(200)} = 0.29$), and (d) fracture surface of direction perpendicular to electric field, poled condition ($I_{(002)}/I_{(200)} = 1.57$).

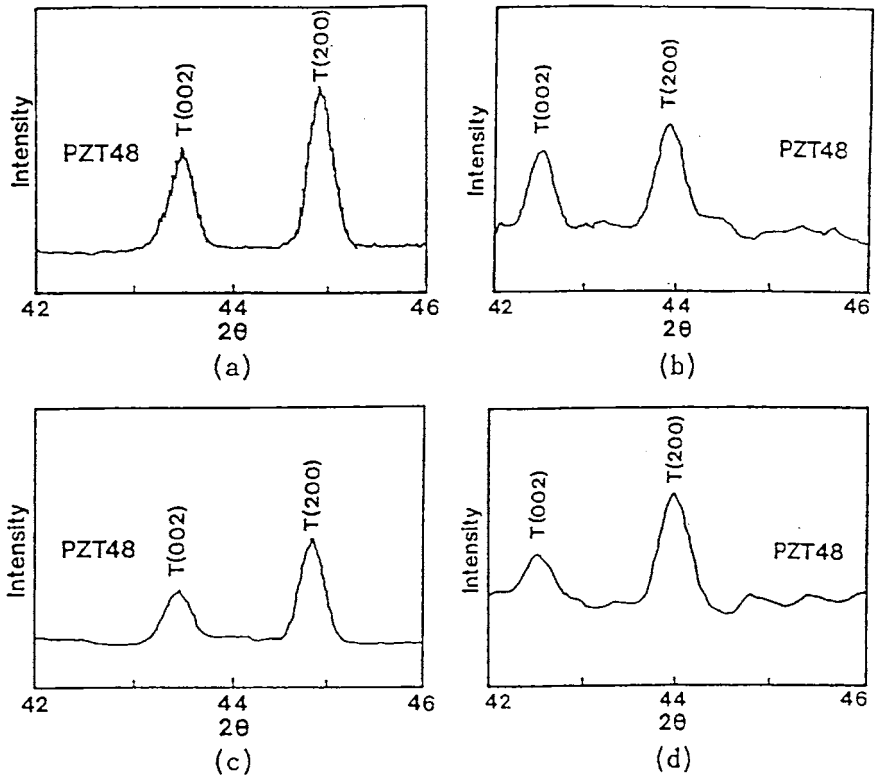

Figure 3 The change in X-ray diffraction patterns of tetragonal $Pb(Zr_{0.48}\ Ti_{0.52})O_3$ before and after poling treatment: (a) surface of unpoled condition ($I_{(002)}/I_{(200)} = 0.67$), (b) fracture surface of unpoled condition ($I_{(002)}/I_{(200)} = 0.85$), (c) surface of direction perpendicular to electric field, poled condition ($I_{(002)}/I_{(200)} = 0.29$), and (d) fracture surface of direction perpendicular to electric field, poled condition ($I_{(002)}/I_{(200)} = 0.4$).

SENB method, the lowest fracture toughness was observed in the tetragonal, while the rhombohedral revealed the highest fracture toughness, as seen in Fig 1. As compared with the SENB method, the indentation strength method [20] showed contrary results for the change in fracture toughness with composition after the poling treatment, as in Fig. 5 where open circles indicate the fracture toughness measured by indentation method [8] and closed circles indicate the fracture toughness measured by indentation strength method [9].

Multiple microcracks around the indentation mark are made in the tetragonal composition during the indentation test. These multiple microcracks relieve or disperse the stress concentration under the 3-point bending load, which results in the reduction of the stress intensity factor at the microcrack tips around the indentation mark. More stress, equivalent to the amount of stress concentration relief owing to the multiplicity of microcracks, is necessary to proceed to fracture. The overestimation of fracture toughness is inevitable in the indentation strength method. Therefore, the effective stress intensity factor acting on a leading crack tip to fracture is greater in the pre-cracked SENB method

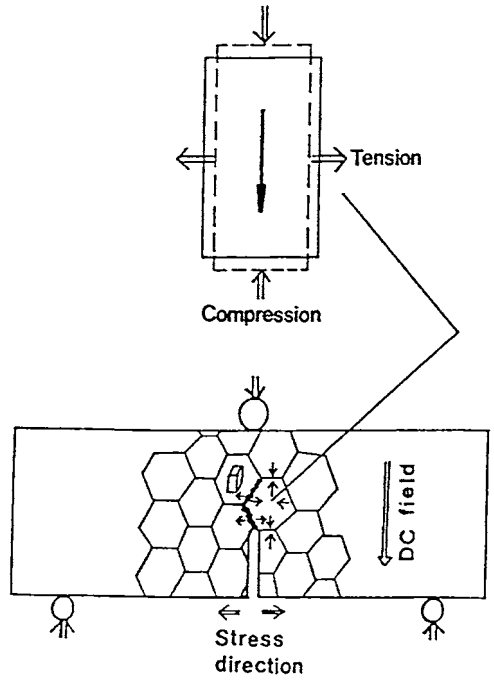

Figure 4 Schematic diagram of stress distribution under 3-point bending loading.

TABLE II Internal stress measured by XRD in PZT ceramics

	PZT 48	PZT 53	PZT 58
Unpoled	−37	91	243
Poled(//)	−1171	−494	−225
Poled(⊥)	217	132	375

Unit: MPa.

than in the indentation strength method, because there is no stress dispersion or relief due to neighbor microcracks in the SENB method. Thus, the specimens under fracture at a lower apparent stress intensity factor in the pre-cracked SENB test.

In an attempt to explain the discrepancy in fracture toughness between the precracked SENB method and the indentation strength method, the stress intensity

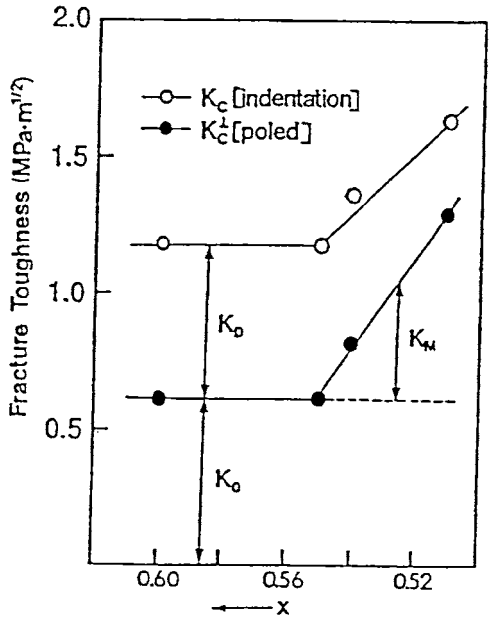

Figure 5 Fracture toughness measured by indentation strength method for various compositions of PZT near MPB [20].

factor values were calculated and presented in Table III for specimens which have multicracks [21] and a single crack [22] as assumed in Fig. 6 for simplicity. It is worth noting that the microcracks in the indentation strength method actually occur radially from the corner of the indentation mark. In order to calculate the stress intensity factor, Equations 2 and 3 were applied for multiple cracks and a single crack, respectively.

$$K_1 = F(a/2t)\sigma a^{1/2} \tag{2}$$

$$K_1 = Pa^{1/2}[1.99 - 0.41(a/w) + 18.7(a/w)^2 - 38.48(a/w)^3 + 53.85(a/w)^4]/[wb\pi^{1/2}] \tag{3}$$

where P is the load, a is the crack length, w is the width of the specimen, $2t$ is the distance between two neighboring cracks, and b is the thickness of the specimen.

For example, if 200 N is applied to a specimen with a crack length of 2.06 mm, the stress intensity factor is 0.358 MPa $\cdot$ m$^{1/2}$ at the crack tip of parallel edge cracks and 1.13 MPa $\cdot$ m$^{1/2}$ at the tip of a single edge crack. In the indentation strength method, the increase in apparent fracture toughness in the tetragonal composition

TABLE III The stress intensity factor values calculated from Bowie [21] and ASTM equation [22] when a 200 N force is applied

Parallel edge crack				Single edge crack			
a (mm)	$a/2t$	p (N)	K_I (MPa·m$^{1/2}$)	a (mm)	a/w	P (N)	K_I (MPa·m$^{1/2}$)
1.23	0.195		0.352	1.23	0.246		0.59
1.49	0.237		0.357	1.49	0.298		0.73
1.76	0.281		0.359	1.76	0.352		0.89
2.06	0.328	200	0.358	2.06	0.412	200	1.13
2.42	0.385		0.359	2.42	0.485		1.52
2.89	0.459		0.360	2.89	0.578		2.28
3.2	0.509		0.355	3.2	0.64		3.04

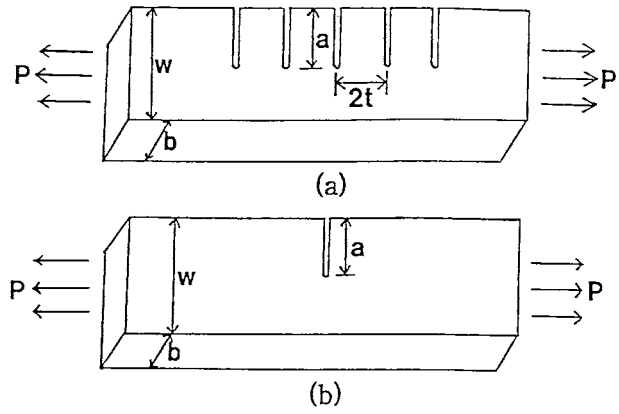

Figure 6 Geometry of specimen: (a) parallel edge crack and (b) single edge crack.

could be attributed to the stress concentration relief owing to the multiple microcracks around the indentation mark while the fracture toughness in the precracked SENB method would be fairly evaluated by the stress concentration at a single crack tip. It is suggested here that fracture toughness testing using the SENB method is preferable, as a standard, to the indentation strength method, because stress concentration at the single crack tip in the precracked SENB method is less variable, while the stress concentration at the multiple microcracks from the indentation mark is difficult to keep consistent.

Cyclic compressive cyclic stress was applied to evaluate fatigue strength and fatigue resistance. The relationship between stress range ($\Delta\sigma$) and fatigue life (N_f) under poled and unpoled conditions is shown in Fig. 7.

For all three compositions, higher fatigue resistance was observed under unpoled conditions than under poled conditions. Before the poling treatment, the fatigue limit was higher in rhombohedral (227 MPa) and MPB (225 MPa) than in tetragonal (131 MPa). Under poled conditions, the highest fatigue limit (227MPa) was also obtained in the rhombohedral composition. Compressive and tensile internal stresses were produced by the poling treatment, as shown in Table II. Higher fatigue resistance in the rhombohedral composition of unpoled samples, as compared with poled ones, resulted from trivial internal stresses due to

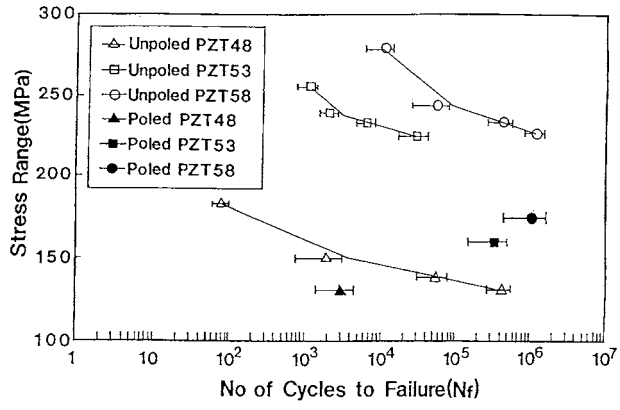

Figure 7 The relationship between stress range and fatigue life for the different PZT compositions.

stable domain arrangement. Higher fatigue resistance in the rhombohedral composition is thought to be attributable to the lower anisotropy of stress distribution, higher density and smaller grain size [19]. The higher anisotropy of internal stress in the tetragonal composition is found to enhance crack propagation when the directions of poling and crack propagation are parallel.

4. Conclusions

The discrepancies in fracture toughness measured by different methods and fatigue strength of piezoelectric PZT were studied before and after poling treatment, and the results are summarized below:

1. Before poling treatment, the highest fracture toughness measured by a single precracked SENB method was observed in the rhombohedral, while the tetragonal showed the lowest fracture toughness. Poling treatment decreased the fracture toughness of PZT in all three compositions. The most prominent decrease in fracture toughness was observed in the tetragonal composition, where the anisotropic internal stress introduced by the domain alignment was parallel to the electric field direction for poling.

2. The discrepancies in fracture toughness values depending on the different measurement methods were explained in terms of the concept of a single crack (in a precracked SENB method) and multiple cracks (in an indentation strength method). Anisotropic internal stresses from the tetragonality which were introduced during the poling treatment were used to explain the extent of the decrease in fracture toughness for the various crystal structures of PZT.

3. Unpoled PZT exhibited higher mechanical fatigue resistance than poled PZT in all three compositions. The highest fatigue resistance among the three compositions was observed in the rhombohedral composition; this was attributed to the lower anisotropy of stress distribution, higher density, and smaller grain size.

Acknowledgement

S. H. Kim thanks Kangwon National University for the financial support that enabled his study leave at the Department of Materials Engineering, Monash University, Australia.

References

1. B. JAFFE, W. R. COOK and H. JAFFE, "Piezoelectric Ceramics" (Academic Press, 1971).
2. S. TAKAHASHI, *Ferroelectrics*, **41** (1982) 143.
3. C. C. M. WU, M. KAHN and W. MOY, *J. Amer. Ceram. Soc.* **79**(3) (1996) 809.
4. S. LATHABAI, Y. W. MAI and B. R. LAWN, *ibid.* **72**(9) (1989) 1760.
5. C. S. YU and D. K. SHETTY, *ibid.* **72**(6) (1989) 921.
6. C. T. FU and A. K. LI, *J. Mater. Sci.* **31** (1996) 4697.
7. R. C. POHANKA, R. W. RICE and B. E. WALKER, *J. Amer. Ceram. Soc.* **59** (1-2) (1976) 71.
8. K. OKAZAKI, *Amer. Ceram. Soc. Bull.* **63**(9) (1984) 1150.
9. S. W. FREIMAN, L. CHUCK, J. J. MECHOLSKY, D. L. SHELLEMAN and L. J. STORZ, in "Fracture Mechanics of Ceramics," edited by R. C. Bradt, A. G. Evans, D. P. H. Hasselman and F. F. Lange Vol. 8 (Plenum Press, New York, 1986) p. 175.
10. K. MEHTA and A. V. VIRKAR, *J. Amer. Ceram. Soc.* **73**(3) (1990) 567.
11. M. J REECE and F. GUIU, *J. Eur. Ceram. Soc.* 21 (2001) 1433.
12. Q. JING, W. CAO and L. E. CROSS, *J. Amer. Ceram. Soc.* **77**(1) (1994) 211.
13. H. CAO and A. G. EVANS, *ibid.* **77** (7) (1994) 1783.
14. L. EWART and S. SURESH, *J. Mater. Sci. Lett.* **5** (1986) 774.
15. S. SURESH, L. EWART, M. MADEN, W. S. SLAUGHTER and M. IVGUYEN, *J. Mater. Sci.* **22** (1987) 1271.
16. M. I. MENDELSON, *J. Amer. Ceram. Soc.* **52**(8) (1969) 443.
17. B. D. CULLITY, "Elements of X-ray Diffraction" (Addison-Wesley, 1978) p. 447.
18. I. C. NOYAN and J. B. COHEN, "Residual Stress Measurements by Diffraction and Interpretation" (Springer-Verlag, 1987) p. 117.
19. W. P. TAI, S. H. KIM and S. H. CHO, *J. Kor. Ceram. Soc.* **29**(10) (1992) 806.
20. S. BAIK, S. M. LEE and B. S. MIN, in "Fracture Mechanics of Ceramics," edited by R. C. Bradt, A. G. Evans, D. P. H. Hasselman and F. F. Lange Vol. 10 (Plenum Press, New York, 1990) p. 371.
21. O. L. BOWIE, in "Methods of Analysis and Solutions of Crack Problems," edited by G. C. Sih (Noordhoff, Holland, 1973).
22. ASTM STP 410, Plane Strain Crack Toughness Testing, 1969.

Received 13 December 2001
and accepted 8 January 2003